

Data Augmentation using Generative Adversarial Networks

Mayur Shastri

University of Massachusetts, Amherst

kshastri@umass.edu

Shreyas Ganesh

University of Massachusetts, Amherst

shreyasganes@umass.edu

Abstract

Modern day deep learning models require massive amounts of data to perform admirably and produce noteworthy results. To this end, we try to resolve this growing need for similarly distributed data and consequently the need for improved Data Augmentation techniques by employing the use of Deep Convolutional Generative Adversarial Networks (DCGANs). We produce new image samples that have similar distributions to the original dataset but can be treated as completely new samples thereby addressing this lack of well distributed data. Our preliminary results show that this DCGAN-based Data Augmentation(DA) method can achieve promising performance improvement, when combined with classical DA, in haemorrhage detection and also in other medical imaging tasks. This study exploits Deep Convolutional GANs (DCGANs), a multi-stage generative training method, to generate original-sized 32 x 32 Head CT images for convolutional neural network-based haemorrhage detection.

1. Introduction

The challenge of obtaining massive amounts of data that is required by modern day deep learning models is one that has intrigued academicians for some time now. This problem is even more prevalent in the medical sphere, where access to high quality medical image datasets is challenging to say the least. Due to licensing and privacy concerns, the need for Data Augmentation in such a space is more necessary. Better training requires intensive Data Augmentation (DA) techniques, such as geometry/intensity transformations of original images. However, these transformed images intrinsically have a similar distribution as the original ones, leading to limited performance improvement. Thus, generating realistic (i.e., similar to the real image distribution) but completely new samples is essential to fill the real image distribution uncovered by the original dataset. To fill the data lack in the real image distribution, we synthesize Head contrast-enhanced Computed Tomography (CT) images—realistic but completely different from the original

ones using Generative Adversarial Networks (GANs). In this context, Generative Adversarial Networks based Data Augmentation(DA) have shown promise as it has shown excellent performances in computer vision, revealing good generalization ability, such as drastic improvement in eye-gaze estimation using SimGAN. [1]

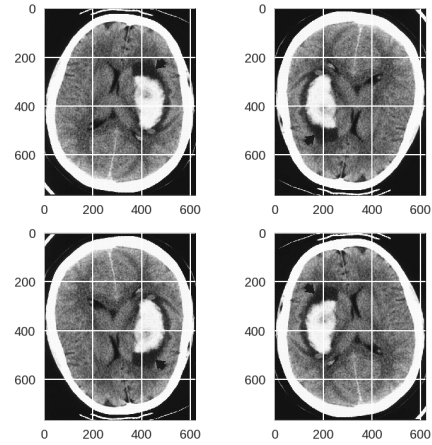


Figure 1. Data Augmentation of CT scans for Haemorrhage Detection

This study exploits Deep Convolutional GANs (DCGANs), a multi-stage generative training method, to generate original-sized 32 x 32 Head CT images for convolutional neural network-based haemorrhage detection. This is quite challenging via other conventional GANs as we discuss below. Difficulties arise due to unstable GAN training with high resolution and a variety of haemorrhage in size, location and shape

In medical imaging, realistic retinal image and Computed Tomography (CT) image generation have been tackled using adversarial learning and as a very recent research [10] reported performance improvement with synthetic training data in CNN-based liver lesion classification, using a small number of 64 x 64 CT images for GAN training. However, GAN-based image generation using CT, the most effective modality for soft-tissue acquisition, has not yet been reported due to the difficulties from low-contrast CT images, strong anatomical consistency, and intrasequence

variability. Previous work [5] has shown that the generated 64 x 64/128 x 128 MR images using conventional GANs and an expert physician failed to accurately distinguish between the real/synthetic images. To generate such highly-realistic and original sized while maintaining clear haemorrhage/non-haemorrhage features using GANs, we first aim to generate GAN-based synthetic head CT images. This can be challenging as

1. GAN training is unstable with high-resolution inputs and severe artifacts appear due to strong consistency in brain anatomy
2. Haemorrhages in the Head CT images vary in size, location, shape, and contrast.

However, it is beneficial, because most CNN architectures adopt around 256 x 256 input sizes and we can obtain better performance with original-sized image augmentation.

2. Related Work

The GAN framework learns two networks (a generator and a discriminator) with competing losses. The goal of the generator network is to map a random vector to a realistic image, whereas the goal of the discriminator is to distinguish the generated from the real images. The GAN framework was first introduced by Goodfellow et al.[6] to generate visually realistic images and, since then, many improvements and interesting applications have been proposed [11].

2.1. Infinite Brain Tumor Images:

Changhee Han et al. [3] exploits Progressive Growing of GANs (PGGANs), a multi-stage generative training method, to generate original-sized 256 x 256 MR images for convolutional neural network-based brain tumor detection, which is challenging via conventional GANs as difficulties arise due to unstable GAN training with high resolution and a variety of tumors in size, location, shape, and contrast. Their preliminary results show that this novel PGGAN-based DA method can achieve promising performance improvement, when combined with classical DA, in tumor detection and also in other medical imaging tasks. We try to replicate the results of this paper for Head Computed tomography (CT) images to for convolutional neural network-based haemorrhage detection.

2.2. Learning More with Less:

This paper [4] introduces GAN-based Medical Image Augmentation, along with tricks to boost classification, object detection and segmentation performance. It also showcases how a GAN-based DA works using automatic bounding box annotation, for robust CNN-based brain metastases

detection on 256 x 256 MR images. Results show GAN-based DA can boost 10 percent sensitivity in diagnosis with a clinically acceptable number of additional False Positives, even with highly-rough and inconsistent bounding boxes.

2.3. Unsupervised Representation Learning

This paper [2] looks to help bridge the gap between the success of CNNs for supervised learning and unsupervised learning. It introduces a class of CNNs called deep convolutional generative adversarial networks (DCGANs), that have certain architectural constraints, and demonstrate that they are a strong candidate for unsupervised learning. Training on various image datasets, we show convincing evidence that our deep convolutional adversarial pair learns a hierarchy of representations from object parts to scenes in both the generator and discriminator. Additionally, we use the learned features for novel tasks demonstrating their applicability as general image representations. This is the model GAN we have used in this paper as well, as it uses convolutional stride and transposed convolution for the downsampling and the upsampling which makes it suitable for our task.

2.4. Improved Training of Wasserstein GANs:

In this paper [7] Ishaan Gulrajani et al. propose an alternative to weight clipping in Wasserstein GAN WGANs which penalizes the norm of gradient of the critic with respect to its input. We adopt the DCGAN architecture with the Wasserstein loss using gradient penalty in this paper. The proposed method performs better than standard WGAN and enables stable training of a wide variety of GAN architectures with almost no hyperparameter tuning, including 101-layer ResNets and language models with continuous generators.

2.5. Brain tumor segmentation with Deep Neural Networks

This paper [8] presents a fully automatic brain tumor segmentation method based on Deep Neural Networks (DNNs). The proposed networks are tailored to glioblastomas (both low and high grade) pictured in MR images. By their very nature, these tumors can appear anywhere in the brain and have almost any kind of shape, size, and contrast. It explores a particularly different architecture based on Convolutional Neural Networks (CNN), i.e. DNNs specifically adapted to image data. It also presents a novel CNN architecture which differs from those traditionally used in computer vision. It also describes a 2-phase training procedure that allows us to tackle difficulties related to the imbalance of tumor/CT image labels.

2.6. Unsupervised Anomaly Detection with Generative Adversarial Networks to Guide Marker Discovery

The paper [12] performs unsupervised learning to identify anomalies in imaging data as candidates for markers. It proposes AnoGAN, a deep convolutional generative adversarial network to learn a manifold of normal anatomical variability, accompanying a novel anomaly scoring scheme based on the mapping from image space to a latent space. Applied to new data, the model labels anomalies, and scores image patches indicating their fit into the learned distribution. The results on optical coherence tomography images of retinal images demonstrate that the approach correctly identifies anomalous images, which in this case were images containing retinal fluid or with hyperreflective foci.

3. Approach

Our approach to solve the growing need for large and robust datasets is to make use of a Deep Convolutional Generative Adversarial Network to generate original-sized 32×32 Head CT images for convolutional neural network-based haemorrhage detection that can be added to the given dataset to produce better results.

Generative Adversarial Networks are actually two deep networks in competition with each other. Given a training set X (say a few thousand images), The Generator Network, $G(x)$, takes as input a random vector and tries to produce images similar to those in the training set. A Discriminator network, $D(x)$, is a binary classifier that tries to distinguish between the real images according to the training set X and the fake images generated by the Generator. As such, the job of the Generator network is to learn the distribution of the data in X , so that it can produce real looking images and make sure the Discriminator cannot distinguish between images from the training set and images from the Generator. The Discriminator needs to learn keep up with the Generator trying new tricks all the time to generate fake images and fool the Discriminator. DCGANs work in a similar fashion except for the fact that they have 2 Convolutional Neural Networks competing against each instead of neural networks.

The our approach first involves pre-processing the images of the given dataset in order to simplify the training of the DCGAN. The next step involves choosing appropriate architectures for the discriminator and generator in order to generate the best possible images. We make use of Convolutional Neural Network(CNN) architectures that are most commonly used for the CIFAR-10 dataset as the CIFAR-10 image resolution is the same as ours. We then train the DCGAN on the preprocessed dataset making use of the chosen discriminator and generator architectures. Finally, we train a ResNet-50 in order to check the effectiveness of our approach. Here we initially train the model with only the orig-

inal dataset and take note of its accuracy and then we train it along with the images generated by the DCGAN. We expect to observe an increase in the accuracy when we make use of the augmented dataset.

4. Experiment

4.1. Dataset Used

This project makes use of a CT Head scan dataset provided by Kaggle. The dataset consists of 200 high resolution images, 100 normal head CT slices and 100 other with hemorrhage. There is no distinction between kinds of hemorrhages. Labels are on a CSV file. Each CT slice comes from a different person. We scaled down the images to $32 \times 32 \times 1$ in order to make it easier to train and to reduce the training time of our model.

4.2. Proposed DCGAN-based Image Generation

4.2.1 Preprocessing:

Since each image in the dataset is only a single slice of a CT scan, we do not have to worry about omitting initial and final slices since all of the information is useful for training the DCGAN and ResNet-50. For haemorrhage detection, our whole dataset (200 patients) is divided into:

- a training set (144 patients)
- a validation set (34 patients)
- a test set (22 patients)

Only the training set is used for the DCGAN training to be fair. The dataset images are hi-res but are scaled down to 32×32 pixels. Hence, training set's images are zero-padded, 32×32 pixels for better DCGAN training. We also make sure that the input images are normalized before they are inputted into the DCGAN. DCGAN is a novel training method for GANs with a deeply convoluted generator and discriminator [8]: starting from low resolution, newly added layers model fine-grained details as training progresses. We adopt DCGANs to generate highly-realistic and original-sized 32×32 head CT images; haemorrhage/non- haemorrhage images are separately trained and generated.

4.2.2 DCGAN Implementation details:

We use a DCGAN architecture with the binary crossentropy loss using gradient penalty. The training goes on for 2500 epochs with a batch size of 16 and a learning rate of 0.0002 and beta equal to 0.5 for the Adam optimizer. We make use of the LeakyRelu activation function except in the following cases:

- The last layer of the discriminator uses a sigmoid activation function.

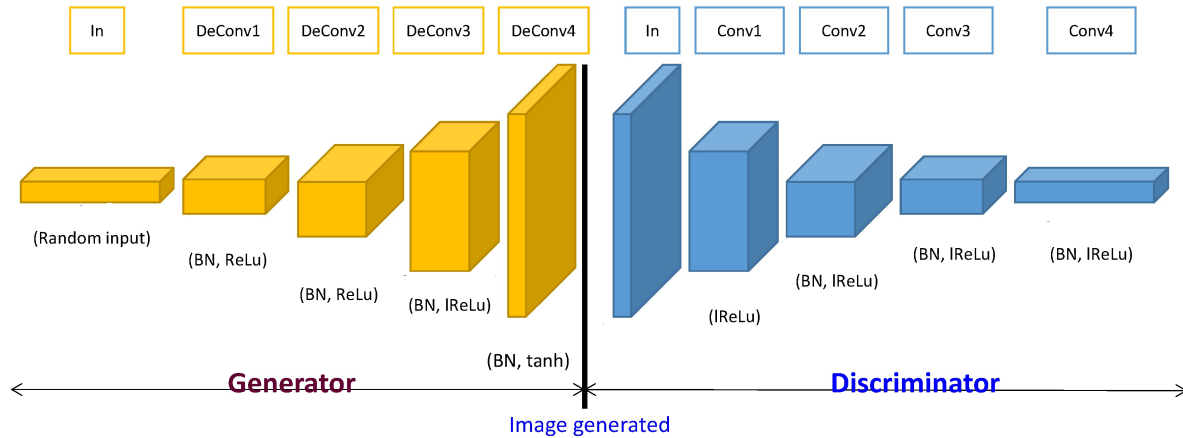


Figure 2. Generator and Discriminator of DCGAN

- The last layer of the generator makes use of the tanh activation function.

Fig 2. Showcases the architecture of the DCGAN implemented in this project for Data Augmentation. This architecture is further expanded upon below. The discriminator of the DCGAN consists of a convolutional neural network with the following architecture:

- Reshape into image tensor (Use Unflatten!)
- Conv2D: 128 Filters, 3x3, Stride 1
- BatchNorm
- Leaky ReLU(alpha=0.01)
- Conv2D: 128 Filters, 3x3, Stride 1
- BatchNorm
- Leaky ReLU(alpha=0.01)
- Conv2D: 128 Filters, 3x3, Stride 1
- BatchNorm
- Leaky ReLU(alpha=0.01)
- Conv2D: 128 Filters, 3x3, Stride 1
- BatchNorm
- Leaky ReLU(alpha=0.01)
- Flatten
- Dropout(0.4)
- Fully Connected with output size 1

The discriminator has a total of 791,169 trainable parameters.

The generator of the DCGAN is also a convolutional neural network with the following architecture:

- Fully connected with output size 128 x 16 x 16
- BatchNorm

- LeakyReLU
- Reshape 16 x 16 x 128
- Conv2D: 128 Filters, 5x5, Stride 1
- BatchNorm
- Leaky ReLU(alpha=0.01)
- Conv2Transpose: 128 filters of 4x4, stride 2, 'same' padding
- BatchNorm
- Leaky ReLU(alpha=0.01)
- Conv2D: 128 Filters, 5x5, Stride 1
- BatchNorm
- Leaky ReLU(alpha=0.01)
- Conv2D: 128 Filters, 5x5, Stride 1
- BatchNorm
- Leaky ReLU(alpha=0.01)
- Conv2D: 128 Filters, 5x5, Stride 1
- BatchNorm
- Leaky ReLU(alpha=0.01)
- TanH
- Should have a 32x32x1 image

The generator has a total of 4,870,785 trainable parameters. Here we make use of the Conv2DTranspose for upsampling. We also make use of techniques like label inversion, real distributed noise etc. in order to improve the performance of the DCGAN.

Once the model has finished training, it is saved as a .h5 file which we then use to generate the images that are used for the Data Augmentation(DA).

4.3. Haemorrhage detection using ResNet50:

The ResNet50 is a deep residual network that was used in this paper to perform binary classification on Head CT images to perform haemorrhage detection. Unlike conventional learning unreferenced functions, it reformulates the layers as learning residual functions for sustainable and easy training. We adopt the ResNet for it's ability to train deep neural networks easily and to prevent accuracy from saturating and degrading.

To fit ResNet-50's input size, we center crop all images from 240×240 to 32×32 pixels. We use the ResNet-50 with a dropout of 0.4 before the final softmax layer, with a batch size of 32. We set the learning rate for the RMS Prop optimizer at 1.0×10^{-3} and used early stopping after 5 epochs.

layer name	output size	18-layer	34-layer	50-layer	101-layer	152-layer
conv1	112×112	7×7 , 64, stride 2				
conv2.x	56×56	3×3 max pool, stride 2				
		$\begin{bmatrix} 3 \times 3, 64 \\ 3 \times 3, 64 \end{bmatrix} \times 2$	$\begin{bmatrix} 3 \times 3, 64 \\ 3 \times 3, 64 \end{bmatrix} \times 3$	$\begin{bmatrix} 1 \times 1, 64 \\ 3 \times 3, 64 \\ 1 \times 1, 256 \end{bmatrix} \times 3$	$\begin{bmatrix} 1 \times 1, 64 \\ 3 \times 3, 64 \\ 1 \times 1, 256 \end{bmatrix} \times 3$	$\begin{bmatrix} 1 \times 1, 64 \\ 3 \times 3, 64 \\ 1 \times 1, 256 \end{bmatrix} \times 3$
conv3.x	28×28	$\begin{bmatrix} 3 \times 3, 128 \\ 3 \times 3, 128 \end{bmatrix} \times 2$	$\begin{bmatrix} 3 \times 3, 128 \\ 3 \times 3, 128 \end{bmatrix} \times 4$	$\begin{bmatrix} 1 \times 1, 128 \\ 3 \times 3, 128 \\ 1 \times 1, 512 \end{bmatrix} \times 4$	$\begin{bmatrix} 1 \times 1, 128 \\ 3 \times 3, 128 \\ 1 \times 1, 512 \end{bmatrix} \times 4$	$\begin{bmatrix} 1 \times 1, 128 \\ 3 \times 3, 128 \\ 1 \times 1, 512 \end{bmatrix} \times 8$
conv4.x	14×14	$\begin{bmatrix} 3 \times 3, 256 \\ 3 \times 3, 256 \end{bmatrix} \times 2$	$\begin{bmatrix} 3 \times 3, 256 \\ 3 \times 3, 256 \end{bmatrix} \times 6$	$\begin{bmatrix} 1 \times 1, 256 \\ 3 \times 3, 256 \\ 1 \times 1, 1024 \end{bmatrix} \times 6$	$\begin{bmatrix} 1 \times 1, 256 \\ 3 \times 3, 256 \\ 1 \times 1, 1024 \end{bmatrix} \times 23$	$\begin{bmatrix} 1 \times 1, 256 \\ 3 \times 3, 256 \\ 1 \times 1, 1024 \end{bmatrix} \times 36$
conv5.x	7×7	$\begin{bmatrix} 3 \times 3, 512 \\ 3 \times 3, 512 \end{bmatrix} \times 2$	$\begin{bmatrix} 3 \times 3, 512 \\ 3 \times 3, 512 \end{bmatrix} \times 3$	$\begin{bmatrix} 1 \times 1, 512 \\ 3 \times 3, 512 \\ 1 \times 1, 2048 \end{bmatrix} \times 3$	$\begin{bmatrix} 1 \times 1, 512 \\ 3 \times 3, 512 \\ 1 \times 1, 2048 \end{bmatrix} \times 3$	$\begin{bmatrix} 1 \times 1, 512 \\ 3 \times 3, 512 \\ 1 \times 1, 2048 \end{bmatrix} \times 3$
	1×1	average pool, 1000-d fc, softmax				
FLOPs		1.8×10^9	3.6×10^9	3.8×10^9	7.6×10^9	11.3×10^9

Figure 3. ResNet Architectures

To confirm the effect of DCGAN-based DA, the following classification results are compared:

- with 200 original images without DA
- with 200 DCGAN-based DA
- with combination of 200 without DA and 200 DCGAN based DA

5. Results

This section shows how the DCGAN generates synthetic head CT images. The results include the various instances of synthetic images and their influence on haemorrhage detection.

5.1. Images Generated by the DCGAN

Fig. 4 illustrates examples of synthetic haemorrhage/non haemorrhage images that have been generated by the DCGAN. From our observations, we noticed that the DCGAN successfully captured texture and appearance of the haemorrhages while maintaining the realism of the original head CT images. However for about 20-25% of the images, we

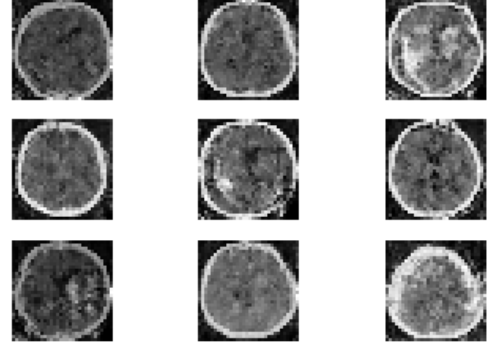


Figure 4. A batch of augmented Head CT images created by our DCGAN

noticed that there was a lack of clarity or unrealistic features. We also assume that even though some of the images have unclear features, they may represent the mean of haemorrhage features which may be useful while training the ResNet-50 (or any other classifier) to accurately classify the head CT images and thus detect haemorrhages in them.

5.2. Haemorrhage detection results (Using ResNet-50)

Table 1 shows the classification results for detecting haemorrhage with/without Data Augmentation. As shown, the test accuracy is around 76.51% when only the original Head CT images were used. When only the DCGAN-based DA images are used, the test accuracy decreases drastically with almost 93.15 of sensitivity and 68.48 of specificity, because the classifier recognizes the synthetic images' prevailed unrealistic features as haemorrhages, similarly to anomaly detection.

However, surprisingly, when a combination of the two are taken, the accuracy of the classifier increases by 2.14% with higher sensitivity and better specificity. Our inference for this occurrence is that the DCGAN-based DA fills the real image distribution uncovered by the original dataset, while the original images provides the robustness on training for most cases.

Fig 5. shows a side by side comparison of the original images and the GAN generated images.

6. Conclusion

The preliminary results of our project show that DCGANs can generate original 32×32 realistic head CT images that can be used to achieve higher performance in haemorrhage detection when combined with classical DA techniques. This is because the images generated by the DCGAN maintain good generalization and synthesizes im-

	Accuracy	Sensitivity	Specificity
ResNet-50 (original)	76.51%	72.37%	83.04%
ResNet-50 (only DA)	60.61%	93.15%	68.48%
ResNet-50 (original + DA)	78.65%	73.14%	86.60%

Table 1. Binary classification results for detecting haemorrhages with/without DA.

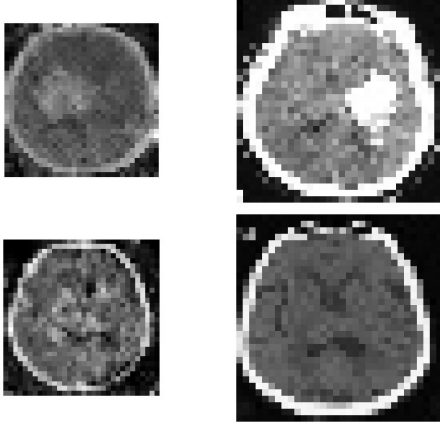


Figure 5. DCGAN Generated Image with Haemorrhage(Top-Left)
Original Image with Haemorrhage(Top-Right)
DCGAN Generated Image without Haemorrhage(Bottom-Left)
Original Image without Haemorrhage(Bottom-Right)

ages which have a distribution unfulfilled by the original dataset.

To evaluate the realism of the generated images, t- Distributed Stochastic Neighbor Embedding (t-SNE) [9] can visualize the distribution of harmorrhage/non-harmorrhage images by extracting the features from the last layer of a trained CNN. However, considering the unsatisfactory realism with high resolution strongly limit DA performance, we plan to

1. discard unrealistic images
2. generate only realistic images
3. refine synthetic images more similar to the real image distribution.

For (1), classifier two-sample tests, assessing whether two samples are drawn from the same distribution, can help discard images not from the real image distribution, as manual removal would be quite demanding. Regarding (2), we can map an input random vector onto each training image and generate images with suitable vectors, to control the divergence of generated images. Lastly, (3) can be achieved by GAN based image-to-image translation, such as CycleGAN [1], considering SimGAN’s remarkable performance improvement after refinement. Moreover, we should further avoid real images with ambiguous/inaccurate annotation for

better haemorrhage detection. Overall, our DCGAN-based DA approach sheds light on diagnostic and prognostic medical applications, not limited to haemorrhage detection but also expandable to tumor detection on MRI images amongst others. We can make use of similar Data Augmentation techniques in other non medical scenarios where one might have limited amounts of data.

We hope that this DA technique combined with classical DA techniques can provide us with even better results than obtained from this project. While our results are heartening, future studies are needed to extend our encouraging results.

References

- [1] O. T. A. Shrivastava, T. Pfister. Learning from simulated and unsupervised images through adversarial training. 2017.
- [2] S. C. Alec Radford, Luke Metz. Unsupervised representation learning with deep convolutional generative adversarial networks. 2016.
- [3] R. A. Y. F. G. M. H. N. H. H. Changhee Han, Leonardo Rundo. Infinite brain tumor images: Can gan-based data augmentation improve tumor detection on mr images? 2018.
- [4] S. S. H. N. Changhee Han, Kohei Murao. Learning more with less: Gan-based medical image augmentation. 2019.
- [5] H. H. R. L. A. R. S. W. M. S. e. a. Han, C. Gan-based synthetic brain mr image generation. 2018.
- [6] M. M. B. X. D. W.-F. S. O. A. C. I. Goodfellow, J. Pouget-Abadie and Y. Bengio. Generative adversarial networks. 2014.
- [7] M. A. I. Gulrajani, F. Ahmed. Improved training of wasserstein gans, proc. conf. on neural information processing systems. 2018.
- [8] D. W.-F. e. a. M. Havaei, A. Davy. Brain tumor segmentation with deep neural networks. 2017.
- [9] L. Maaten and G. Hinton. Visualizing data using t-sne. 2018.
- [10] E. K. M. A. J. G.-a. H. G. Maayan Frid-Adar, Idit Diamant. Gan-based synthetic medical image augmentationfor increased cnn performancein liver lesion classification. 2018.

- [11] W. Z. V. C.-u. A. R. T. Salimans, I. Goodfellow and X. Chen. Improved techniques for training gans. 2016.
- [12] S. M. W.-e. a. T. Schlegl, P. Seebock. Unsupervised anomaly detection with generative adversarial networks to guide marker discovery. 2017.